Preparation of Agarose-based Biopolymer Electrolytes Containing Calcium Thiocyanate: Electrical and Electrochemical Properties

N. S. Mohd Rafi[1], S. Z. Z. Abidin[1,2,*], S. R. Majid[3,*], R. Zakaria[1,2]

[1] Faculty of Applied Sciences, Universiti Teknologi MARA, 40450 Shah Alam, Selangor, Malaysia;
[2] Ionic Materials and Devices (iMADE) Research Laboratory, Institute of Science, Universiti Teknologi MARA, 40450 Shah Alam, Selangor, Malaysia;
[3] Centre for Ionics University of Malaya, Department of Physics, Faculty of Science, University of Malaya, 50603, Kuala Lumpur, Malaysia;
[*]E-mail: szafirah@uitm.edu.my; shana@um.edu.my

CaSCN─agarose biopolymer electrolytes were prepared by infusing various amounts of CaSCN salts (0–40 wt.%) in 0.5 g of agarose. CaSCN─agarose biopolymer electrolytes had been prepared through a solution casting technique and had been kept in the oven for 36 h at the temperature range of ~ 80 ºC before the film form. The characterization technique included the electrical conductivity, structural and electrochemical properties of calcium-conducting biopolymer electrolytes in the frame of reference to match with universal needed for electrochemical devices in high energy storage appliances. The prepared electrolytes were characterized by electrical impedance spectroscopy (EIS) to study the electrical behaviour of the electrolytes at room temperature and temperature dependence. The highest conducting sample, 40 wt.% CaSCN─agarose biopolymer electrolytes resulted in a favourable ionic conductivity value of 8.01×10^{-05} S.cm$^{-1,}$ and all prepared samples of CaSCN─agarose biopolymer electrolytes obey Arrhenius behaviour. The ionic conduction mechanisms were presented in detail by dielectric studies and modulus studies. The molecular interactions between agarose polymer and CaSCN salts were further affirmed in fourier transform infrared spectroscopy (FTIR) studies and the results highlighted the presence of C─O─C, ─OH, ─CH, ─CC, ─NH and SCN anions. The maximum ionic conductivity value was successfully supported by X-Ray diffractometry (XRD), declared 40 wt.% CaSCN─agarose biopolymer electrolytes as the highest amorphicity due to the reduction of crystalline peaks at $2\theta = 19°–22°$ and showed the lowest percentage of crystallinity, 31.81 % that calculated from deconvolution process. Electrochemical studies by linear sweep voltammetry (LSV) recorded that CaSCN─agarose biopolymer electrolytes resulted in a favourable electrochemical stability window at 2.9 V, and the result was supported by Cyclic Voltammetry (CV) analysis, and study paves in the fostering calcium conducting biopolymer electrolytes as a promising separator in calcium batteries.

1. INTRODUCTION

Rising energy demand for high technology power supply leads to the advancement in the field of polymer electrolytes, and researchers continuously produce alternatives to improve recent polymer electrolytes in the aspects of ionic conductivity, durability, mechanical stability, and biodegradability [1]. Biodegradable materials have been chosen to satisfy the contribution towards Fourth Industrial Revolution with clean energy that focuses on green technologies to solve the challenges such as air pollution and oil dependency among our modern society [2].

Previous studies report that calcium ions, Ca^{2+} are one of the divalent ions that gained attention in the research of electrolytes systems because of high availability, reasonable price and safe handling [3]. Calcium is the fifth most abundant material in earth's crust, and its potential of standard reduction (0.17 V) above lithium is able to produce the more considerable cell potential [4], Ca^{2+} possess a faster kinetic reaction over other divalent elements such as magnesium ions, Mg^{2+} due to its lower polarizing behaviour and enable to produce gain up to 300 % in energy storage density [5].

In developing calcium ion-based energy storage technologies, it is crucial to study more profound aspects of electrical behaviour such as ionic conductivity, ion transport mechanism and potential stability in their electrolyte selection. High ions dissociation at the electrode-electrolyte interface is required to ensure the good ionic conductivity of the system. However, previous studies declare that determining the suitable electrolyte for divalent ions is quite challenging, especially for calcium [5]. Theoretically, the strength of cations interaction of divalent ions and the anions reactions are essential for designing a new divalent ions-based electrolyte system that can produce a multivalent ion-based battery [5]–[8]. However, the advancement of calcium ion-based electrolytes is slower because Ca^{2+} has slow diffusion in the active material, and it produces a low working voltage which is approximately below 2.0 V [3]; thus, studies on calcium ion-based electrolytes are limited. A frequent challenge in research on calcium ion-based is the formation of a passivation layer between the calcium electrode and the electrolytes. Aurbach and his group was the earliest found passivation layer on the calcium metal electrode [9]. They found that when CaO, $CaCO_3$, and $Ca(OH)_2$ are in contact with organic solvents, a solid electrolyte interface (SEI) is formed and causes Ca^{2+} blocking. This phenomenon prevents calcium ions access to the underlying bulk [10–11]. Therefore, this work reported the first attempt using agarose as a polymer host for calcium ion conduction to solve the blocking issues. The hydroxyl group promotes the Ca^{2+} ions conduction, containing an electronegative atom (oxygen) in the repeating unit of agarose.

Research in electrolytes currently focuses on natural polymers such as agarose, chitosan, phytagel, starch, cellulose and gelatin to replace the synthetic polymers that give adverse long-term effects to the environment [11]–[13]. This report focuses on the use of agarose as a polymer matrix in calcium ions-based electrolytes because it has yet to be discovered. Although naturally, agarose is one of the polysaccharides family obtained from the extraction of red marine algae (Agarophyta), agarose is mainly composed of a disaccharide as a repeating unit with strong gel-forming properties [15–16].

In this work, calcium thiocyanate (CaSCN) salts incorporated with agarose as a polymer host were used to produce calcium-based biopolymer electrolytes. The electrolytes systems were undergoing several characterizations such as electrical impedance spectroscopy (EIS), fourier transform infrared spectroscopy (FTIR), X-Ray diffraction (XRD), linear sweep voltammetry (LSV) and cyclic

Int. J. Electrochem. Sci., 17 **(2022)** Article Number: 220713

3

voltammetry (CV) was conducted to verify the electrical and electrochemical performance of CaSCN─agarose biopolymer electrolytes.

2. METHODOLOGY

2.1. Materials

Biopolymer agarose (molecular weight, M_w: 630.5 g.mol^{-1}) was procured from Next Gene (Malaysia). Calcium thiocyanate tetrahydrate (CaSCN) (Sigma-Aldrich, 95%) functioned as dopant and dissolved by dimethyl sulfoxide (DMSO) (M_w: 256.41 g.mol^{-1}, ≥99.7%) obtained from Fisher Scientific. All chemicals were used upon receiving in preparation of CaSCN─agarose biopolymer electrolytes.

2.2 Agarose based electrolytes films

Desired amounts of 0–40 wt.% CaSCN salts (5 wt.% intervals) and 0.5 g of agarose were dissolved in 20 mL of DMSO under stirring until a clear solution was formed. Next, CaSCN─agarose biopolymer electrolytes were cast onto the petri dish before being kept in the oven for 36h in the temperature range (70–80 ° C) for a drying process. Agarose successfully formed a good quality and a clear standalone film with an average thickness of 0.005–0.014 cm, as shown in Figure (1).
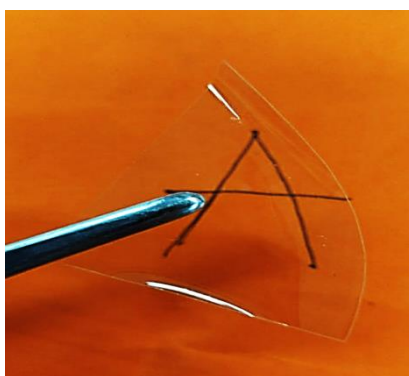
Figure 1. A clear thin film of CaSCN─agarose biopolymer electrolyte.

2.3 Electrical Impedance Spectroscopy

CaSCN─agarose biopolymer electrolytes samples were cut into small pieces, and the samples were sandwiched between two stainless steel. HIOKI 3532-50 LCR Hi-tester from 300 K to 373 K was used to measure the impedance at 100 Hz to 1 MHz of the frequency range. The ionic conductivity of the electrolytes was calculated from this equation (1).

$$\sigma = \frac{t}{R_b A} \tag{1}$$

Whereby σ is the DC conductivity, t is the thickness of CaSCN─Agarose biopolymer electrolytes, A is the surface area contact and bulk resistance, R_b. Bulk resistance was obtained from the impedance plot, specifically at the interception between the semicircle at low frequency and the incline spike at high frequency on the real impedance axis. Through EIS analysis, samples were tested at room temperature and temperature dependence from 303 K to 373 K while placing the samples in the humidity chamber to avoid external humidity. Samples were placed carefully between the electrodes to ensure the best contact of the electrode-electrolyte interface, resulting in more accurate EIS test results.

2.4 Fourier Transform Infrared Spectroscopy

Identification of the molecular interaction of the electrolyte systems obtained by fourier transform infrared spectroscopy (FTIR) analysis. The spectrum showed the interaction between CaSCN salts and polymer agarose in the biopolymer electrolytes system. Measurement of the spectra referred from the absorption of infrared radiation that identified specific characteristics of components and structures of electrolytes. In this study, FTIR spectra were recorded using Perkin Elmer model 400 spectrum with the range of spectral between 450 and 4000 cm^{-1} with 4 cm^{-1} resolutions.

2.5. X-Ray Diffraction

The structural appearance of the CaSCN─agarose biopolymer electrolytes are completely crucial as supporting evidence that the system could exhibit better performance in terms of amorphousity. Therefore, X-Ray diffraction (XRD) spectra were analyzed based on monochromatic X-rays' constructive interference and a crystalline sample. The Bragg angle, 2θ in XRD diffractometer was varied from 5° to 90° at room temperature, and the highest peak in XRD spectra interpreted the degree of crystallinity of CaSCN─agarose biopolymer electrolytes using PANalytical X'pert PRO diffractometer with CuK$_\alpha$ radiation (**λ**= 1.5418 Å).

2.6. Electrochemical Measurement

2.6.1 Linear Sweep Voltammetry

Linear sweep voltammetry (LSV) analysis obtained by Automatic Battery Cycler, model WBCS 3000, WonA Tech, Seoul, South Korea. The electrode potential is varied at a constant rate during the analysis, and the resulting current is measured. Change in current with varying voltage express the plot known as voltammogram. In LSV, voltage is scanned from the lower limit to the upper limit, and voltage scan rate is calculated from the slope of the potential line. Characteristics of LSV depends on the rate of electron transfer reaction, chemical reactivity in the gel polymer electrolytes system and voltage scan rate. Scanning started from the left-hand side of the current/voltage plot where there is no current flow. As the voltage swept to the right to the more reductive value, the current started to flow and reach the maximum peak before dropping. The voltage range is performed from -1.8 V–3.0 V using these electrode

configurations, stainless steel (SS) as a working electrode and calcium foil as counter and reference electrodes. CaSCN—agarose biopolymer electrolytes serve as a separator between those two electrodes to avoid short circuits.

2.6.2. *Cyclic Voltammetry*

Cyclic voltammetry (CV) test was conducted with scan rate 5 mV.s^{-1} between -1.8 V and 4.0 V in the same electrode configuration as LSV analysis, SS//CaSCN—agarose//Ca. CV analysis helped to investigate the chemical reaction by electron transfer in CaSCN—Agarose biopolymer electrolytes.

3. RESULTS AND DISCUSSION

### 3.1 *Electrical impedance spectroscopy*

The impedance plots (Z_i vs Z_r) of CaSCN—agarose biopolymer electrolytes at different concentrations of CaSCN salts at room temperature are portrayed in Figure 2(a—f), where bulk resistance (R_b) plots in the figure satisfied two main components, semicircle at high-frequency part and inclined spike at low-frequency part. The semicircle is visible at 15 wt.% in Figure 2(a) and invisible insight when the weight percent of CaSCN salts increase. The semicircle attributed to the ionic conducting properties of CaSCN—agarose biopolymer electrolytes and the incline spike corresponded to the double-layer capacitance behaviour due to blocking ions at the end of blocking electrodes [18]. The situation occurs at the end of the blocking electrode, known as the polarization effect at the electrode-electrolyte interface [2–19]. Figure 3(a) depicts the ionic conductivity values for (0–45 wt.%) of CaSCN—agarose biopolymer electrolytes at room temperature. Since the ionic conductivity values are calculated according to equation (1), it is found that the ionic conductivity increases with the increment of CaSCN salts concentration. Pure CaSCN—agarose biopolymer electrolyte results in the ionic conductivity value of 1.07×10^{-08} S.cm^{-1}, which shows that polymer agarose is the best choice for host polymer as it satisfies the conductivity ranges for pure polysaccharides biodegradable materials from ~10^{-14} to 10^{-8} S.cm^{-1} [11]. The increment of ionic conductivity values depends on the hopping mechanism in CaSCN—agarose biopolymer electrolytes that occurs when Ca^{2+} ions continuously diffuse in the agarose polymer matrix and attach to the oxygen lone pair provided by hydroxyl and carboxyl group from the matrix and produce polyionic bonding [16] as shown in Figure 3(b). The ionic conductivity value increases until it reaches the desired value of 8.01×10^{-05} S.cm^{-1} at 40 wt.% CaSCN salts concentration, the increment of conductivity values occurs due to the high density of Calcium ions as the charge carriers and the increment of mobile charge species (Ca^{2+} cations and SCN^{-1} anions) in CaSCN—agarose biopolymer electrolytes' membrane [17,20–22]. The ionic conductivity value is still high at 45 wt.% where the value is 2.28×10^{-04} S.cm^{-1}.

However, the structure of the electrolytes become weak as 45 wt.% CaSCN—agarose biopolymer electrolytes unable to withstand temperature above 353 K. This statement is supported by the temperature dependence analysis illustrated in Figure 3(c). The linear variation of plots in this study is considered to obey Arrhenius behaviour, where the conductivity increases due to the temperature

increment. Arrhenius behaviour of the CaSCN—agarose biopolymer electrolytes is further amplified with the regression value, R^2 for the linear plot of log σ versus 1000/T, which is almost unity. Adding CaSCN salts introduces the new coordinating sites for the Ca^{2+} cations to jump from one coordination site to another after an electric field is applied. The graph interprets that the temperature influences the ionic conductivity of CaSCN—agarose biopolymer electrolytes, which can be related to the Arrhenius rule by equation (2).

$$\sigma = \sigma_0 \exp \frac{-E_a}{k_B T} \tag{2}$$

Where σ_o refers to the pre-exponential factor, E_a and K_B is the value of activation energy and Boltzmann constants respectively. Thermal energy weakens the ion's re-dissociation during the solvent drying process and promotes more free ions for the conduction mechanism in CaSCN—agarose biopolymer electrolytes. Thus it enhances the conductivity value at high temperatures [17]. The activation energy of the selected samples (0 wt.%, 15 wt.% and 40 wt.%) of CaSCN—agarose biopolymer electrolytes are determined to be 0.107 eV, 0.199 eV and 0.069 eV respectively. The low activation energy value proposes that the ion mobility in the CaSCN—agarose biopolymer electrolytes membranes is effortless, where the ions freely move and promote high ionic conductivity due to the abundance of the charge carriers. In addition, it supports the structure of an optimum conducting sample, 40 wt.% CaSCN—agarose biopolymer electrolytes are more amorphous where it facilitates the quick Ca^{2+} cations motion [18]. The reduction in activation energy value is the factual agreement that the amount of ions increase due to the decrement of the energy barrier to the ion transport [19].
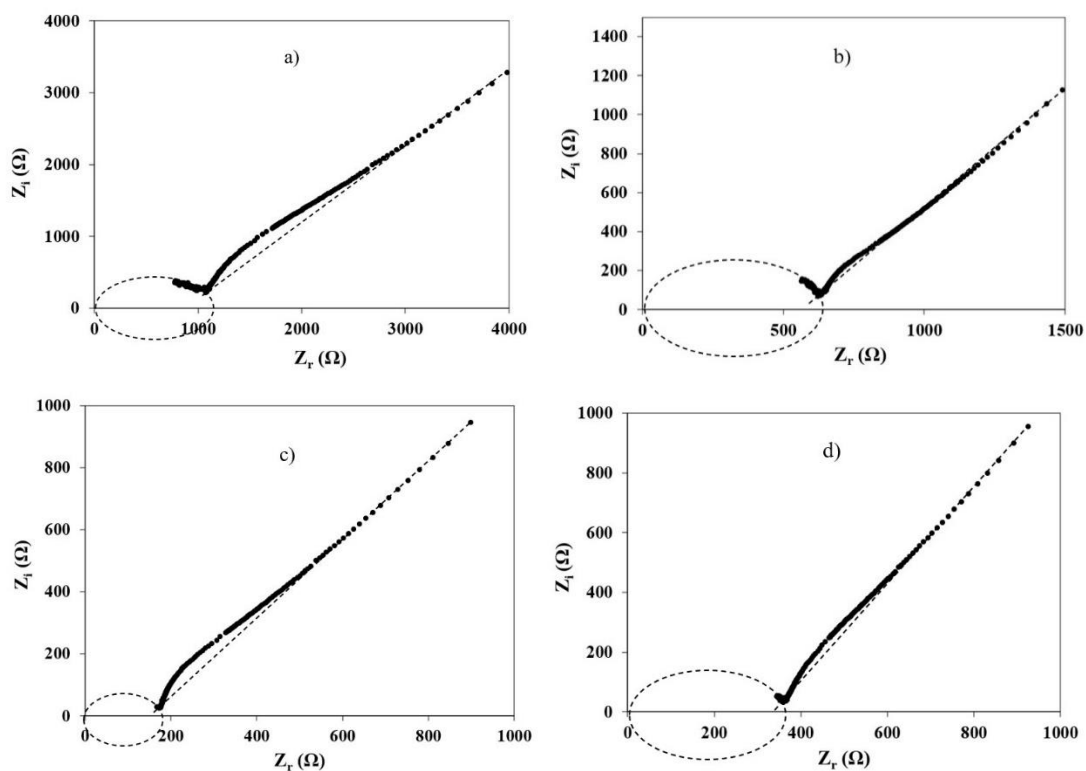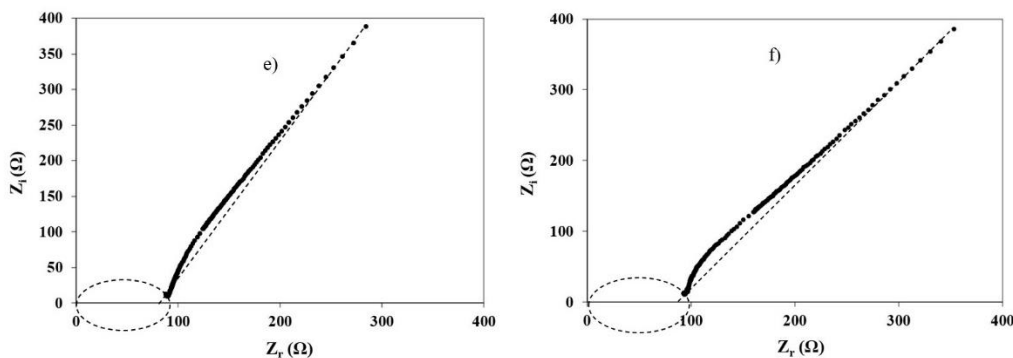
Figure 2. Impedance plots for (a) 15 wt.% (b) 20 wt.% (c) 25 wt.% (d) 30 wt.% (e) 35 wt.% (f) 40 wt.% CaSCN─agarose biopolymer electrolytes.
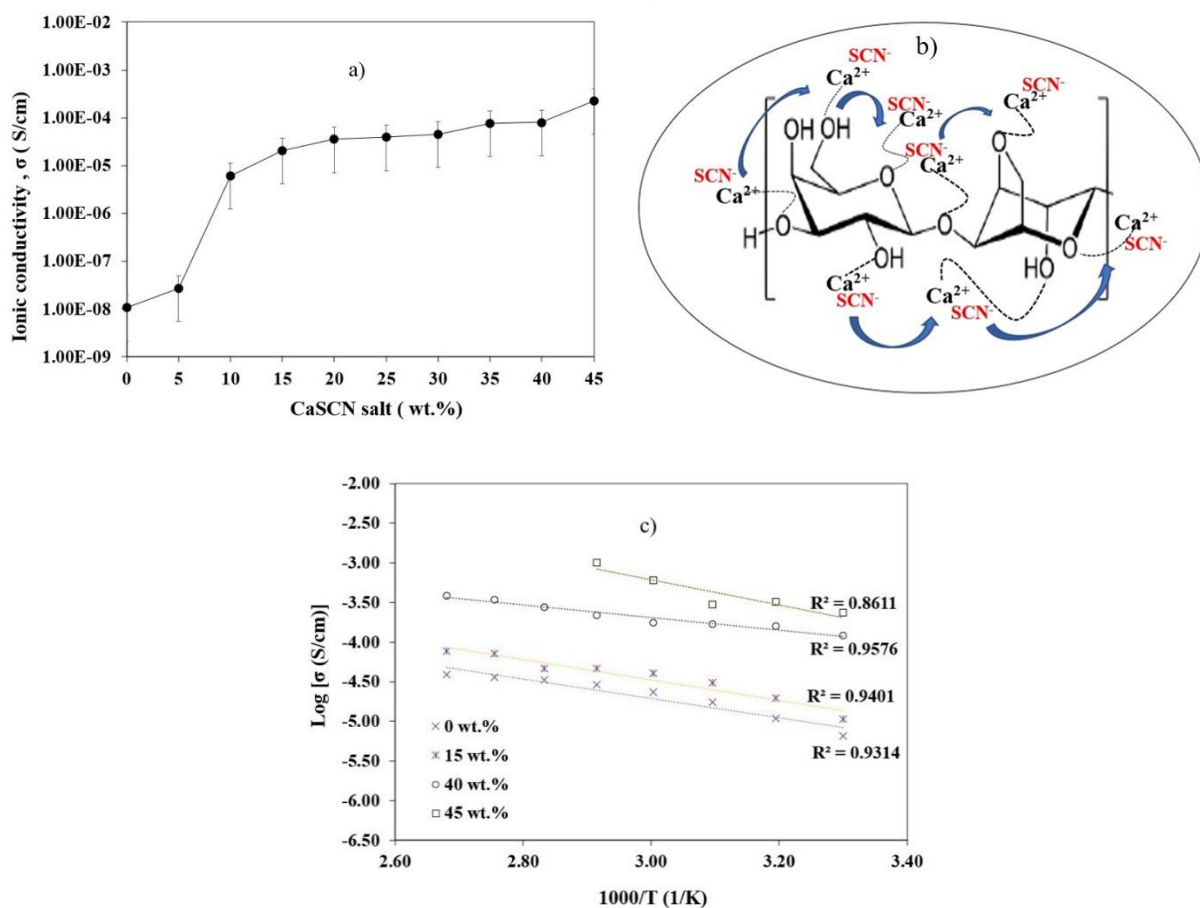
Figure 3. (a) Ionic conductivity of different amounts of CaSCN salt at room temperature, (b) Hopping mechanism of Ca^{2+} in CaSCN─agarose biopolymer electrolytes, (c) Temperature dependence plots of different concentration of CaSCN─agarose biopolymer electrolytes.

3.2 Dielectric study

Dielectric properties help understand ion transportation and relaxation processes that practically explain CaSCN-agarose biopolymer electrolytes' conductivity behaviour. The results are analyzed by

calculating the permittivity using the impedance data from the temperature dependence part. Real permittivity, ε_r known as dielectric storage or the ability of CaSCN–agarose biopolymer electrolytes to store charge while imaginary permittivity or dielectric loss, ε_i acknowledge the energy losses due to the ion migration found in the electrode-electrolyte interface. The information is compacted into the following equation:

$$\varepsilon_r = \frac{Z_r}{\omega C_o(Z_r^2 + Z_i^2)} \tag{3}$$

$$\varepsilon_i = \frac{Z_i}{\omega C_o(Z_r^2 + Z_i^2)} \tag{4}$$

C_o equal to $\varepsilon_o A/t$ and ε_o is the permittivity of free space (8.8542×10^{-12} m^{-3} kg^{-1}s^4 A^2). Z_r and Z_i represent real and imaginary impedance, respectively.

Figures 4(a) and 4(b) portray the dependence of the frequency of ε_r and ε_i at ambient temperature for 40 wt.% CaSCN–agarose biopolymer electrolytes. Consequent to the increase in temperature, it triggers the mobility of Ca^{2+} cations and signifies the free movement of the cations, then enhances the store charged in the electrolyte's membrane. Rising of ε_r values with increasing temperature at low frequencies due to the movement of Ca^{2+} free ions along the field before confines by the blocking electrode and the ions assemble at the electrode-electrolyte interface to form an electrical double layer [17]. The electric field's reversal rate increases accordingly with the increasing temperature prevents the charges from building up at the interface [20]. ε_r values slowly decrease before becoming sluggish at high temperatures are caused by the electrode polarisation [21]. Figure 4(b) describes the increment of ε_i with increasing temperature as it experiences great molecular relaxation, and the values become higher at low-frequency caused by the accumulation of charge carriers, Ca^{2+} cations and resulting in the thin layer of capacitance[22], [23]. Further understanding in relaxation mechanism is strengthened by the formulism of dielectric modulus which real modulus, M_r and imaginary modulus, M_i which expressed as below:

$$M_r = \frac{\varepsilon_r}{(\varepsilon_r^2 + \varepsilon_i^2)} \tag{7}$$

$$M_i = \frac{\varepsilon_i}{(\varepsilon_r^2 + \varepsilon_i^2)} \tag{8}$$

ε_r and ε_i represent dielectric storage and dielectric loss, respectively.

Modulus studies illustrate by the plots of M_r and M_i against a frequency of 40 wt.% CaSCN–agarose biopolymer electrolytes as shown in Figures 4(c) and 4(d), respectively. Modulus properties result from the bulk effect in the electrolytes system. They acquire a strong relationship with both dielectric constant and dielectric loss. It is observed that the value of the real modulus is approximate zero at the lower frequency region, which means the contribution of electrode polarization is negligible. The long tail at lower frequency indicates the long-range ionic motion and small modulus values associated with the high capacitance that causes the electrode polarization to be neglected [32].

Modulus plots shift towards higher frequency values with increasing temperature due to reducing relaxation time. Theoretically, to confirm that the electrolyte system is an ionic conductor, a peak must be observed in imaginary modulus plots, but in the present case, the peak in imaginary plots is absent. The issues might be because the temperature range is not wide enough, and the conductivity does not depend too much on temperature [24].
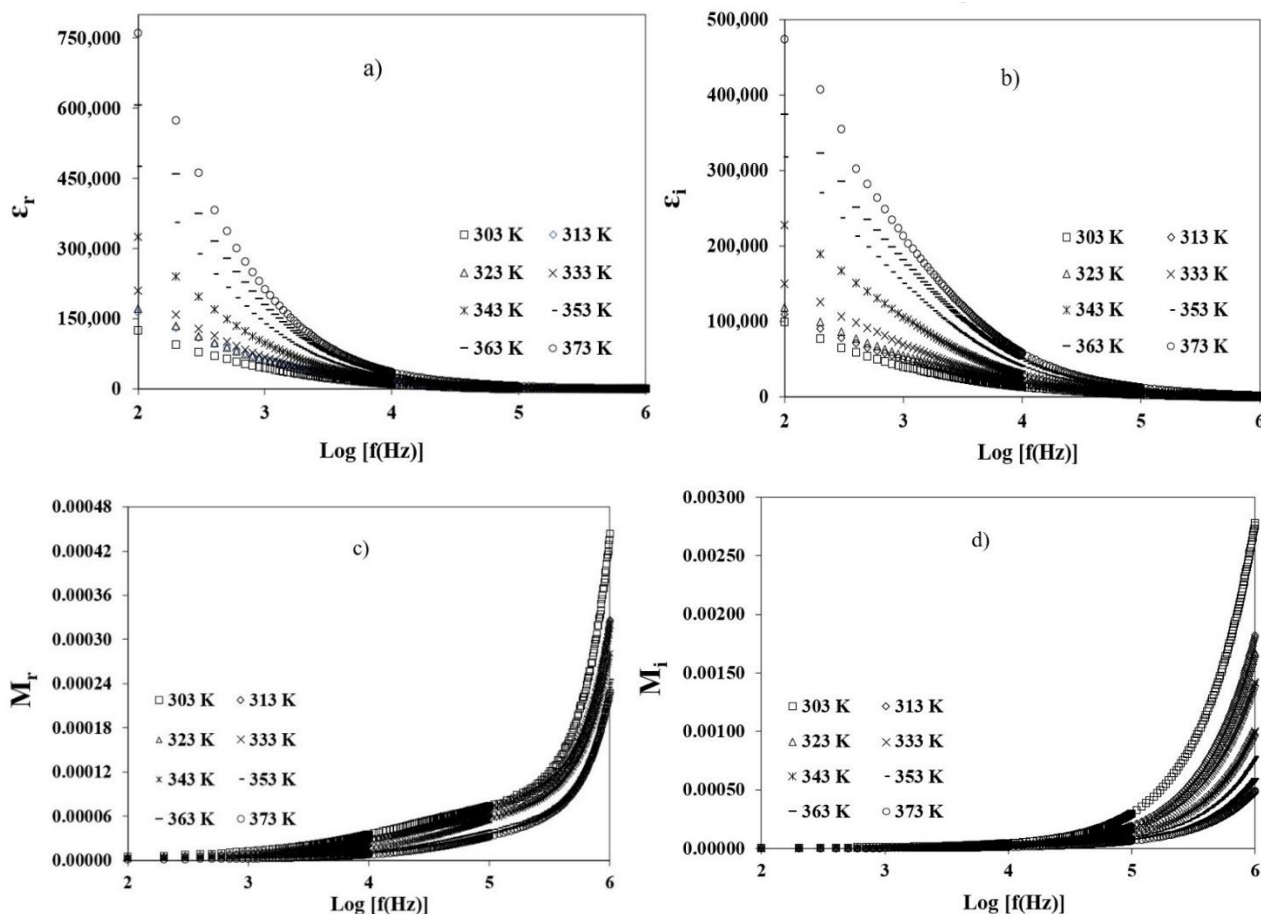
Figure 4. Electrical properties of CaSCN─agarose biopolymer electrolytes (a) Dielectric storage, (b) Dielectric loss, (c) Real modulus, (d) Imaginary Modulus.

### 3.3 Fourier Transform Infrared Spectroscopy

Molecular interaction from the incorporation of agarose biopolymer and CaSCN salts help in strengthening the understanding of the ionic conduction mechanism of CaSCN─agarose biopolymer electrolytes. Figure 5(a), 5(b) portrays the infrared spectrum at specific bonding of pure agarose and infrared spectrum of CaSCN─agarose biopolymer electrolytes films. There are several significant peaks belonging to the pure agarose, which centred at 932 cm^{-1} due to 3,6-anhydrogalactose bending [13], [17], [25], [26], 1067 cm^{-1} belongs to C─OH stretching [27], and 1154 cm^{-1} attributes to C─O─C stretching vibration [13], [17].

In addition, the peaks observe at 1373 cm^{-1}, 1643 cm^{-1}, 2907 cm^{-1}, 3364 cm^{-1} are assigned to the CH$_3$ bending, H—O—H stretching vibrations [15], [25], [26], C—H stretching vibrations [27], O—H stretching vibrations [13], [27], respectively. Figure 4(b) observes a significant change in the FTIR spectra with the addition of CaSCN salts at different concentrations. The addition of CaSCN salts shifts the 3,6-anhydrogalactose bending to 966 cm^{-1}, region (i). Strong C—OH vibrations observe at a higher wavenumber at 1069 cm^{-1} –1073 cm^{-1} as stated in the region (ii). The wavenumbers of C—O—C at region (iii), 1154 cm^{-1} –1158 cm^{-1} corresponds to the presence of carbohydrates units [17], [28]. In another report region (iv) at wavenumber from 1580 cm^{-1} to 1650 cm^{-1} is related to N—H bending and C=O group [16], [29]. There is no solid evidence to state the specific band properties for CaSCN salts however, the SCN^{-1} anions assignment band is available at a strong intensity of 2069 cm^{-1} at region (v) [30]. The peaks own by SCN^{-1} is directly proportional to the salt's concentration because of the increasing density of ions dissociation. The prominent peaks for aggregates ions are clearly observed at higher wavenumber at region (vi), 3370 cm^{-2} –3390 cm^{-1} due to the strong pairing of Ca^{2+} cations and SCN^{-1} anions.

The overlapping complex spectra in the region 1525 cm^{-1}–1725 cm^{-1} that refers to the carbonyl group (C=O) for several samples of CaSCN—agarose biopolymer electrolytes are deconvoluted to high sensitivity and Gaussian Lorentzian peak type using Origin Pro8 software. In addition, baseline correction has been done to all deconvolution, the solid line corresponds to the experimental data, and the red dash line refers to the curve-fitting line. This technique examines the ion dissociations and the transportation of charge carriers, Ca^{2+}.

The overlapping peaks are assumed to cause by the hopping mechanism of Ca^{2+} ions with the C=O group, and the assignments of the peaks have been simplified in Table 1. Ca^{2+} ions hopping at oxygen atoms increase upon the increasing concentration of CaSCN salts in the electrolytes system because of the increment of charges carrier density in the polymer matrix. The absorption group of C=O appears in two types: free C=O and hydrogen-bonded C=O. It happens when the groups interact with N—H and O—H, also known as proton donating groups [31].

The deconvolution process in Figure 6(a–e) analyses the peaks' behaviour where the peaks are shifted to the higher wavenumber with increasing CaSCN salts concentration because the mechanism provides higher energy vibration. The area of the peaks become bigger as the salts increase, thus high charge carrier density (Ca^{2+}) and more interaction between the cations with the oxygen lone pair at C=O groups. Area of Ca^{2+} bonded C=O for selected CaSCN—agarose biopolymer electrolytes (0 wt.%, 10 wt.%, 20 wt.%, 30 wt.% and 40 wt.%) are identified from the curve fitting of deconvolution process, and the plot area under the peak of Ca^{2+} bonded C=O against CaSCN contents is portrayed in Figure 7. The observation from the curve area shows the area is expanding with salts concentration. Therefore, it reinforces the knowledge of enhancing ionic conductivity up to 40 wt.% CaSCN salts concentration is dominantly caused by the increases in the number of Ca^{2+} ions coordinated with the C=O bands.
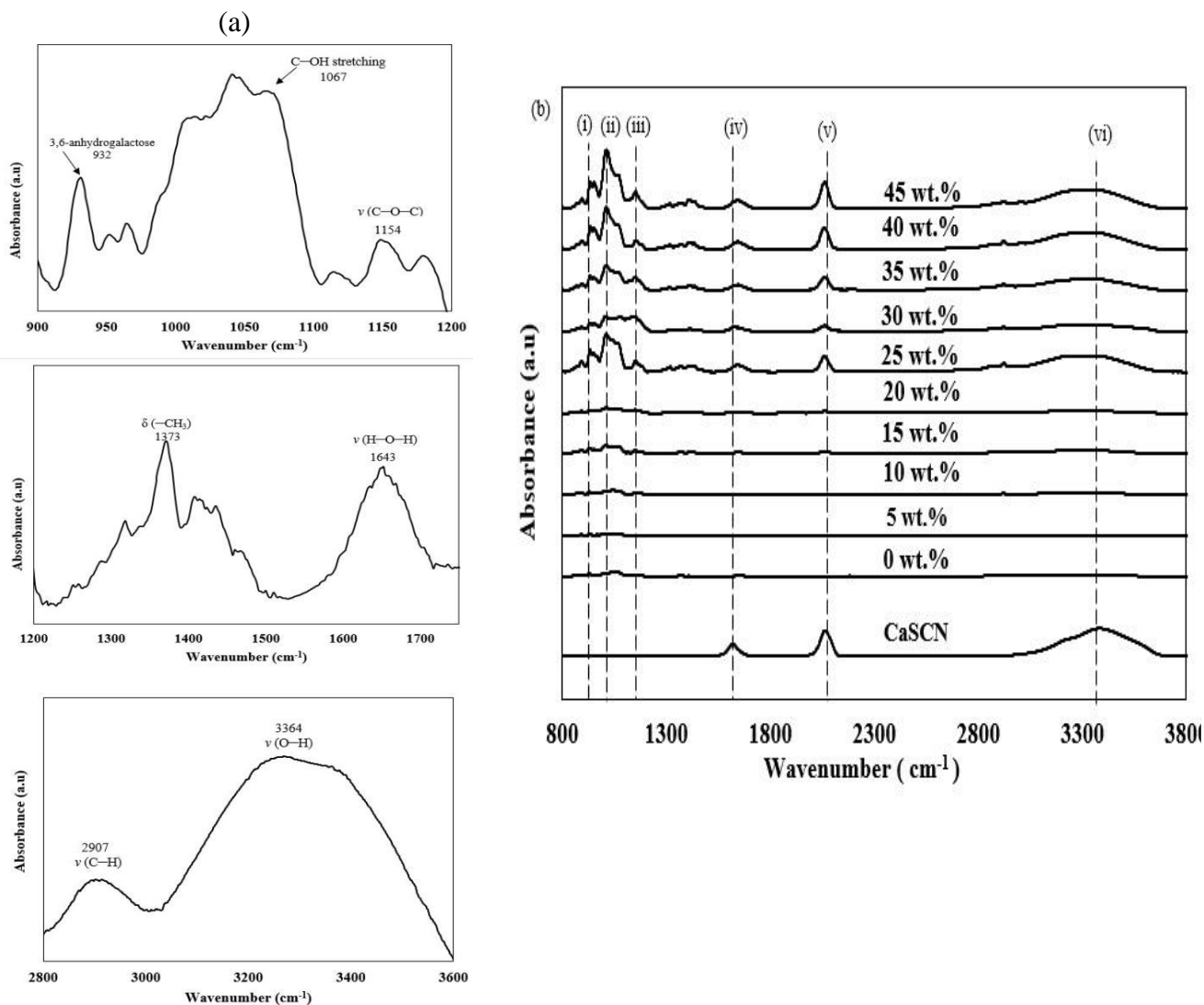
Figure 5. (a) Significant peaks for pure agarose　(b) FTIR spectrum for pure CaSCN salt and CaSCN─agarose biopolymer electrolytes' system.

Table 1. Lists of important peaks in the FTIR spectrum of CaSCN─agarose biopolymer electrolytes system.

| No.	Wavenumber (cm^{-1})	Assignment bands	References
(i)	940–966	O─H stretching	[16], [30]
(ii)	1069–1073	C=O stretching vibration	[30]
(iii)	1154–1158	C─O stretching C─C stretching	[13], [16], [30]
(iv)	1580–1650	N─H bend C=O stretching vibration	[16], [29]
(v)	2069	SCN^{-1} anions	[39]
(vi)	3370–3390	Ion pairs of Ca^{2+} cations and SCN^{-1} anions	
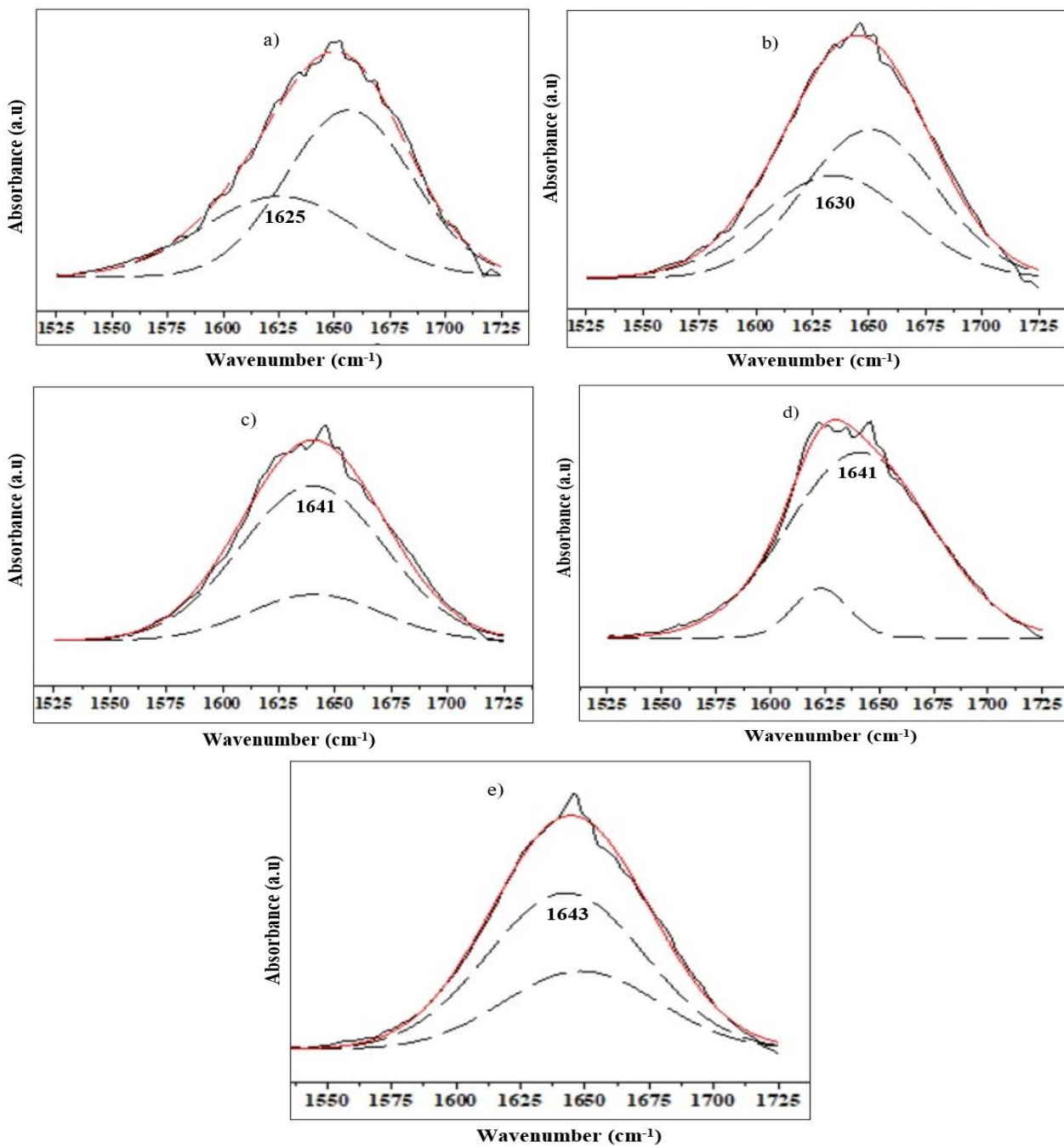
Figure 6. Deconvolution at C=O region within range 1525 cm^{-1} to 1725 cm^{-1} for several weight percent of CaSCN─agarose biopolymer electrolytes. (a) 0 wt.%, (b) 10 wt.%, (c) 20 wt.%, (d) 30 wt.%, e) 40 wt.%
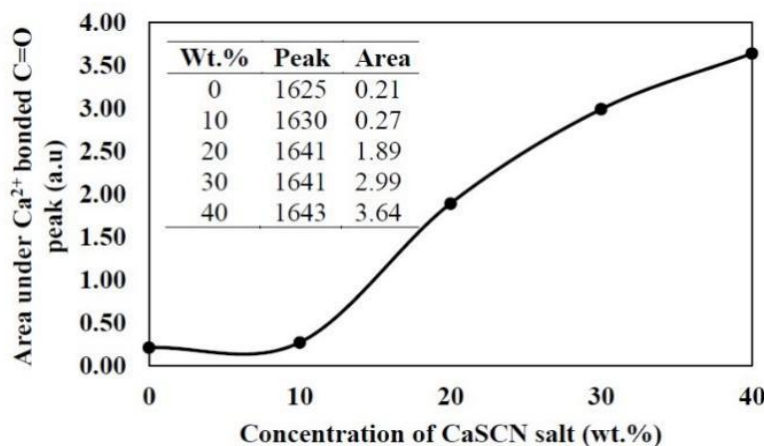
Figure 7. The area under peak Ca^{2+} bonded C=O as a function of CaSCN concentration in selected CaSCN─agarose biopolymer electrolytes.

3.4 X-ray diffraction studies

X-Ray Diffraction (XRD) has been carried out to affirm further the effect of CaSCN salts in the structure of agarose polymer. X-ray diffractogram of pure CaSCN salts, pure agarose powder as well as the system of CaSCN─agarose biopolymer electrolytes are shown in Figure 8 (a), (b). The recorded X-ray diffraction pattern of CaSCN salts show several prominent peaks at $2\theta = 20.78°$, $21.61°$, $23.07°$, $29.82°$, $37.13°$, $44.32°$, and $44.35°$. The sharpness and high intensity of the diffraction peaks clearly show the good crystallinity of the salts [32].
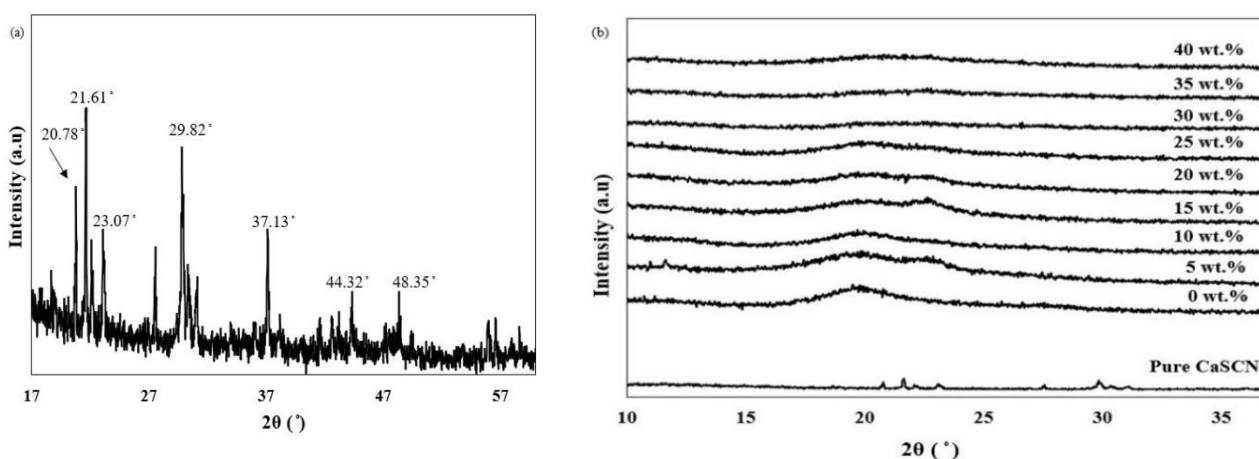
Figure 8. (a) Diffractogram of pure CaSCN, (b) XRD spectrum of CaSCN─Agarose biopolymer electrolytes system.

Incorporation of CaSCN salts with agarose polymer in the CaSCN-Agarose biopolymer electrolytes system suppresses the intense crystalline peaks of the salts, the absence of the peaks indicates the complete dissolution of salts in the polymer matrix. The diffraction pattern for pure agarose show a broad hump at $2\theta = 15°-30°$ and previous studies [16], [33], [34] reported that these peaks are known as

the semi-amorphous nature of agarose film. The decrement of broadening hump upon adding 5 wt.% to 40 wt.% of CaSCN salts indicates that the systems increase their amorphous region and produce a favourable condition for ionic conductivity enhancement [33]. However, there are appearances of two peaks when the salts coordinate into the agarose polymer matrix, and they might cause by the incomplete dissolution of CaSCN salts biopolymer electrolyte films [30].

The intensity of the hump is a noticeable decrease, and it has been confirmed through XRD deconvolution technique by Gaussian function in Figure 9 (a–d) at range $2\theta = 13°$–$37°$ to specify the character of the existence peaks. Referring to the deconvolution pattern in the figures, the crystalline peak that appears at range $2\theta = 19°$ to $22°$ seem to be more broadened upon increasing the salts concentration. The highest conducting sample, 40 wt.% CaSCN salt confirms its characteristic as the most favourable sample due to the broadest amorphous hump. High amorphicity eases the path for the ions migration and mobility in the electrolyte, increasing conductivity value. The peak was slightly absent in 40 wt.% CaSCN–agarose biopolymer electrolyte indicates the complete dissociation of salts in the electrolytes [35]. The dominance of the amorphous region is mathematically confirmed by calculating the degree of crystallinity (X_c) using *equation (9)* and the crystallite size, L using *equation (10)*:

$$X_c = \frac{A_c}{A_a + A_c} \times 100 \tag{9}$$

Where A_C refers to the area of crystalline peak and A_a corresponds to the area of the amorphous peak of the sample.

$$L = \frac{0.9\,\lambda}{FWHM \cos\theta} \tag{10}$$

Where L is the crystallite size, **λ** is the fixed X-Ray diffraction wavelength, 1.5406 Å, FWHM stands for full width half maximum observed from the peak broadness and Braggs' diffraction angle, θ.

The percentage of crystallinity of 0 wt.%, 10 wt.%, 25 wt.%, and 40 wt.% CaSCN–agarose biopolymer electrolytes are tabulated in **Table 2**. The results show the high amorphous nature, the lowest degree of crystallinity, and the smallest crystallite size obtained by 40 wt.% CaSCN–agarose biopolymer electrolytes, 31.81 % and 2.75×10^{-11} m.
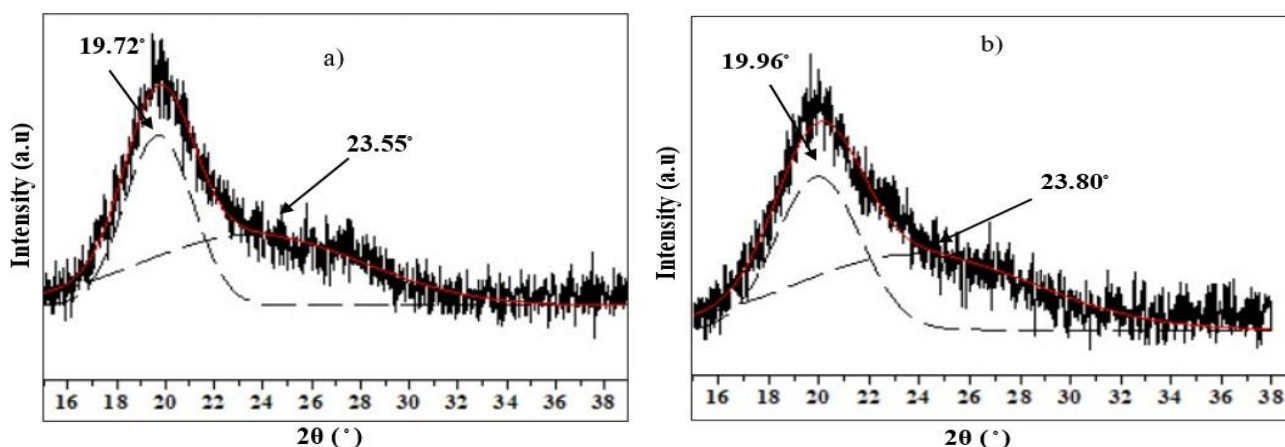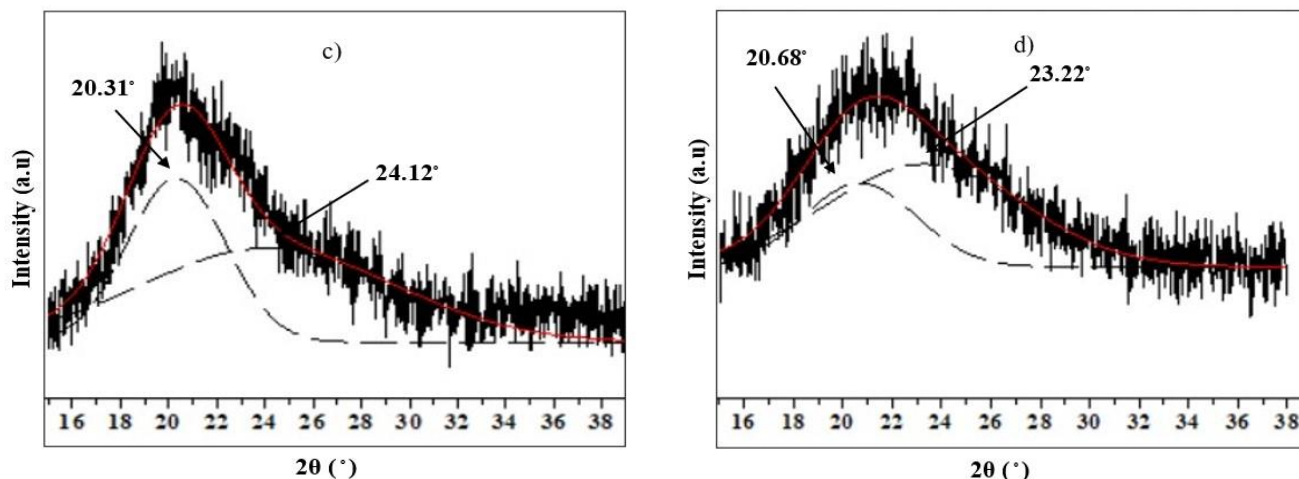
Figure 9. Deconvolution for several weight percent of CaSCN—agarose within range 13° and 37° at room temperature. (a) 0 wt.%, (b) 10 wt.%, (c) 25 wt.%, and (d) 40 wt.

Table 2. The degree of crystallinity, X_c and crystallite size, L of selected CaSCN—agarose biopolymer electrolytes (wt.%)

Amount of CaSCN salts (wt.%)	Degree of crystallinity, X_c (%)	FWHM	Crystallite size, L ($\sim 10^{-11}$ m)
0	43.11	3.2881	4.49
10	41.87	3.9424	3.74
25	40.20	4.8075	3.08
40	31.81	5.3930	2.75

3.5 Electrochemical analysis

        In order to delineate the promising performance of the CaSCN—agarose biopolymer electrolyte in the calcium electrochemical system, **t**he electrochemical stability of the biopolymer film was studied by measuring LSV and CV. The tested coin cell was assembled from the configuration consisting of stainless steel/biopolymer film/Ca metal foil and swept from -1.8 to 3 V (vs. Ca/Ca^{2+}) at ambient temperature, Figure 10(a). There is limited electrochemical stability reported on calcium ion-based polymer electrolytes because of the lack of feasibility of electrolytes incorporated with the calcium [36]. In the LSV profile**,** the electrolyte film exhibited a good electrochemical stability window. The plot evidenced that the electrolyte film has decomposed after the voltage exceeds +1.8 V which is surmised to become up from the oxidation of functional groups or oxide decomposition in the polymer and caused to the unstable system. The result satisfies the standard voltage potential value for a proton battery, 1.0 V [31,32] and is promising to be applied in other electrochemical devices such as calcium ion-based batteries. In the CV profile, Figure 10(b) with Ca metal as the counter and reference electrode, the observed anodic peak at ~1.9 and 2.4 V in Figure 10(c) conform to the Ca stripping, which strongly implies the Ca conduction has occurred. A weak cathodic shoulder-like feature in Figure 10(d) is recorded at ~-1.17 V vs Ca counter electrode, which can be inferred to the Ca plating onto the SS

working electrode. Indeed, the observed plating/stripping peaks corroborate that the CaSCN—agarose biopolymer electrolyte allows the ions to balance in the cell.
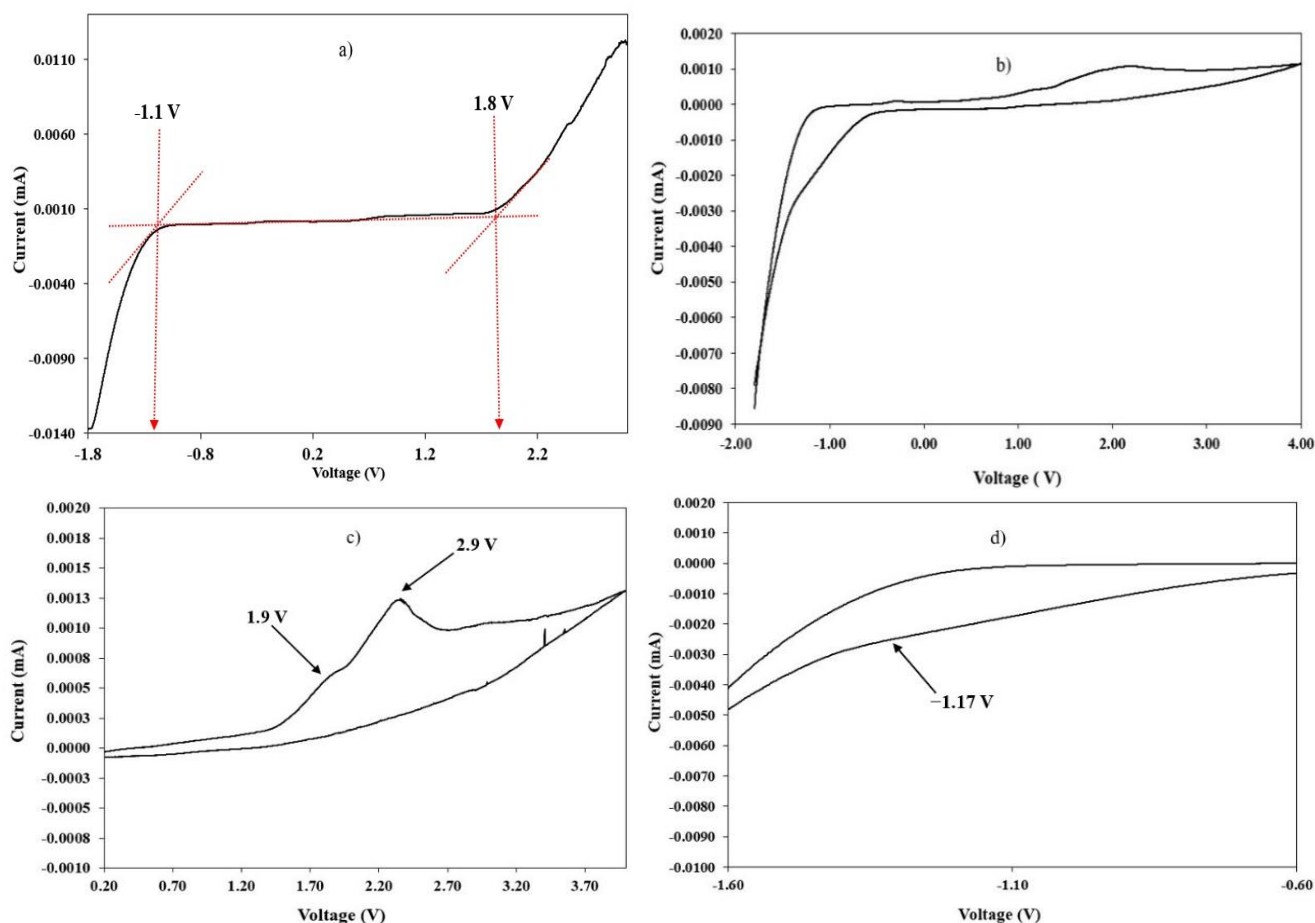
Figure 10. Electrochemical studies of the highest conducting film (a) Linear sweep voltammetry and (b) Cyclic voltammetry (scan rates 5 mV.s^{-1}), (c) Anodic peak, (d) Cathodic shoulder peak.

4. CONCLUSION

According to the result obtained in this present work, the value of ionic conductivity increases with increasing salts and 40 wt.% CaSCN—agarose exhibits the highest value of conductivity, 8.01×10^{-5} S.cm^{-1} at room temperature and resulting in the lowest activation energy at 0.069 eV. The ionic conductivity of CaSCN—agarose biopolymer electrolytes is found to be influenced by the Ca^{2+} ions that serve as the charge carrier in the electrolytes system. Temperature dependence analysis proves the system at (0–40 wt.%) CaSCN contents can withstand up to 373 K, however at 45 wt.% CaSCN only able to reach up to 353 K due to the weakness of the structural properties. FTIR studies are achievable to explain the presence of C—O—C, —OH, —CH, —CC, —NH and SCN anions in the CaSCN—agarose biopolymer electrolytes system. The highest area under deconvoluted Ca^{2+} bonded C=O is achieved by 40 wt.% CaSCN—agarose biopolymer electrolytes indicate the most interactions between Ca^{2+} with C=O, enhancing the ionic conductivity value. Structural analysis by XRD verifies the broaden of the

crystalline peak from 2θ =19 ° to 22 °, and the best sample provides the most amorphous nature of the electrolytes system where 40 wt.% CaSCN─agarose biopolymer electrolytes have the smallest percent of crystallinity and the smallest crystallite size. High amorphicity in the structure of CaSCN─agarose biopolymer electrolytes promotes ions' mobility, thus increasing ionic conductivity. CaSCN─agarose biopolymer electrolytes achieved a good electrical performance by LSV and CV characterization where the potential stability window is 2.9 V above the standard potential value, thus making CaSCN─agarose biopolymer electrolytes is applicable in the use of calcium batteries.

References

1.   N. Kulshrestha and P. N. Gupta, *Nature*, 22 (2015) 671.
2.   H. J. Woo, S. R. Majid, and A. K. Arof, *Solid State Ionics*, 199 (2011) 14.
3.   S. Wu, F. Zhang, and Y. Tang, *Adv. Sci.*, 5 (2018) 1.
4.   A. Ponrouch, C. Frontera, F. Bardé, and M. R. Palacín, *Nat. Mater.*, 15 (2015) 1.
5.   S. H. Lapidus, N. N. Rajput, X. Qu, K. W. Chapman, K. A. Persson, and P. J. Chupas, *Phys. Chem. Chem. Phys.*, 16 (2014) 21941.
6.   H. S. Kim, T. S. Arthur, G. D. Allred, J. Zajicek, J. G. Newman, A. E. Rodnyansky, A. G. Oliver, W. C. Boggess, and J. Muldoon, *Nat. Commun.*, 2 (2011) 426.
7.   Q. Zhao, Y. NuLi, T. Nasiman, J. Yang, and J. Wang, *Int. J. Electrochem.*, 2012 (2012) 1.
8.   P. Wang, Y. NuLi, J. Yang, and Z. Feng, *Surf. Coatings Technol.*, 201 (2006) 3783.
9.   A. M. Melemed and B. M. Gallant, *J. Electrochem. Soc.*, 167 (2020) 140543.
10.   D. Aurbach, R. Skaletsky, and Y. Gofer, *J. Electrochem. Soc.*, 138 (1991) 3536.
11.   V. L. Finkenstadt, *Appl. Microbiol. Biotechnol.*, 67 (2005) 735.
12.   V. Sahu, R. B. Marichi, G. Singh, and R. K. Sharma, *ACS Sustain. Chem. Eng.*, 5 (2017) 8747.
13.   R. M. Felfel, M. J. Gideon-Adeniyi, K. M. Zakir Hossain, G. A. F. Roberts, and D. M. Grant, *Carbohydr. Polym.*, 204 (2019) 59.
14.   P. L. Lam, K. K. H. Lee, S. H. L. Kok, G. Y. M. Cheng, X. M. Tao, D. K. P. Hau, M. C. W. Yuen, K. H. Lam, R. Gambari, C. H. Chui, and R. S. M. Wong, *Soft Matter.*, 8 (2012) 5027.
15.   T. J. Trivedi, D. Bhattacharjya, J. Yu, and A. Kumar, *ChemSusChem*, 8 (2015) 3294.
16.   R. Singh, B. Bhattacharya, S. K. Tomar, V. Singh, and P. K. Singh, *Measurement*, (2017).
17.   N. I. Ali, S. Z. Z. Abidin, S. R. Majid, and N. K. Jaafar, *Polymers (Basel, Switz.)*, 13 (2021) 3357.
18.   N. H. Zainol, S. M. Samin, L. Othman, K. B. Isa, W. G. Chong, and Z. Osman, *Int. J. Electrochem. Sci.*, 8 (2013) 3602.
19.   R. Leones, F. Sentanin, L. C. Rodrigues, I. M. Marrucho, J. M. S. S. Esperança, A. Pawlicka, and M. M. Silva, *Express Polym. Lett.*, 6 (2012) 1007.
20.   A. S. A. Khiar and A. K. Arof, *Ionics*, 16 (2010) 123.
21.   R. Singh, P. K. Singh, V. Singh, and B. Bhattacharya, *Cellul. Chem. Technol.*, 51 (2017) 949.
22.   S. B. Aziz, M. A. Brza, K. Mishra, M. H. Hamsan, W. O. Karim, R. M. Abdullah, M. F. Z.

Kadir, and R. T. Abdulwahid, *J. Mater. Res. Technol.*, 9 (2020) 1137.
23.   M. A. Brza, S. B. Aziz, H. Anuar, E. M. A. Dannoun, F. Ali, R. T. Abdulwahid, S. Al-Zangana, and M. F. Z. Kadir, *Polymers (Basel, Switz.)*, 12 (2020) 1.
24.   M. Kumar, T. Tiwari, and N. Srivastava, *Carbohydr. Polym.*, 88 (2012) 54.
25.   F. Topuz, A. Nadernezhad, O. S. Caliskan, Y. Z. Menceloglu, and B. Koc, *Carbohydr. Polym.*, 201 (2018) 105.
26.   Z. Hu, P. Hong, M. Liao, S. Kong, N. Huang, C. Ou, and S. Li, *Materials (Basel)*, 9 (2016) 1.
27.   W. Wang, X. Guo, and Y. Yang, *Electrochim. Acta*, 56 (2011) 7347.
28.   Y. Wang, C. Li, P. Liu, Z. Ahmed, P. Xiao, and X. Bai, *Carbohydr. Polym.*, 82 (2010) 895.
29.   I. Der Wu and F. C. Chang, *Polymer (Guildf)*, 48 (2007) 989.
30.   R. Hemalatha, M. Alagar, S. Selvasekarapandian, B. Sundaresan, and V. Moniha, *J. Sci. Adv. Mater. Devices*, 4 (2019) 101.
31.   A. Arya, M. Sadiq, and A. L. Sharma, *Mater. Today Proc.*, 12 (2019) 554.
32.   U. Er, K. C. Icli, and M. Ozenbas, *J. Solid State Electrochem.*, 24 (2019) 293.
33.   R. Singh, B. Bhattacharya, H. W. Rhee, and P. K. Singh, *Int. J. Hydrogen Energy*, 40 (2015) 9365.
34.   S. R. Majid and A. K. Arof, *Phys. Status Solidi A.*, 2401 (2007) 2396.
35.   A. Arya and A. L. Sharma, *J. Phys. Condens. Matter.*, (2018) 1.
36.   A. Ponrouch and M. P. Rosa, *Curr. Opin. Electrochem.*, 9 (2018) 1.
37.   N. A. M. Noor and M. I. N. Isa, *Int. J. Hydrogen Energy*, 44 (2019) 8298.
38.   R. Pratap, B. Singh, and S. Chandra, *J. Power Sources*, 161 (2006) 702.